

Design and fabrication of a bending rotation fatigue test rig for in situ electrochemical analysis during fatigue testing of NiTi shape memory alloy wires

Lakshman Neelakantan, Jenni Kristin Zglinski, Matthias Frotscher, and Gunther Eggeler

Citation: *Rev. Sci. Instrum.* **84**, 035102 (2013); doi: 10.1063/1.4793488

View online: <http://dx.doi.org/10.1063/1.4793488>

View Table of Contents: <http://rsi.aip.org/resource/1/RSINAK/v84/i3>

Published by the [American Institute of Physics](http://www.aip.org).

Additional information on *Rev. Sci. Instrum.*

Journal Homepage: <http://rsi.aip.org>

Journal Information: http://rsi.aip.org/about/about_the_journal

Top downloads: http://rsi.aip.org/features/most_downloaded

Information for Authors: <http://rsi.aip.org/authors>

ADVERTISEMENT

For all your variable temperature, solid state characterization needs....
... delivering state-of-the-art in technology and proven system solutions for over 30 years!

MMR TECHNOLOGIES

Solutions for Optical Setups!

Seebeck Measurement Systems

Variable Temperature Microprobe Systems

Hall Measurement Systems

Email: sales@mmr-tech.com Web: www.mmr-tech.com Phone: (650) 962-9622 Fax: (888) 522-1011

Design and fabrication of a bending rotation fatigue test rig for *in situ* electrochemical analysis during fatigue testing of NiTi shape memory alloy wires

Lakshman Neelakantan,^{1,2,a)} Jenni Kristin Zglinski,¹ Matthias Frotscher,^{1,3} and Gunther Eggeler¹

¹Ruhr-Universität Bochum, Institute for Materials, 44801 Bochum, Germany

²Department of Metallurgical and Materials Engineering, Indian Institute of Technology Madras, 600 036 Chennai, India

³CORTRONIK GmbH, 18119 Rostock-Warnemuende, Germany

(Received 19 July 2012; accepted 11 February 2013; published online 5 March 2013)

The current investigation proposes a novel method for simultaneous assessment of the electrochemical and structural fatigue properties of nickel-titanium shape memory alloy (NiTi SMA) wires. The design and layout of an *in situ* electrochemical cell in a custom-made bending rotation fatigue (BRF) test rig is presented. This newly designed test rig allows performing a wide spectrum of experiments for studying the influence of fatigue on corrosion and vice versa. This can be achieved by performing *ex situ* and/or *in situ* measurements. The versatility of the combined electrochemical/mechanical test rig is demonstrated by studying the electrochemical behavior of NiTi SMA wires in 0.9% NaCl electrolyte under load. The *ex situ* measurements allow addressing various issues, for example, the influence of pre-fatigue on the localized corrosion resistance, or the influence of hydrogen on fatigue life. *Ex situ* experiments showed that a pre-fatigued wire is more susceptible to localized corrosion. The synergetic effect can be concluded from the polarization studies and specifically from an *in situ* study of the open circuit potential (OCP) transients, which sensitively react to the elementary repassivation events related to the local failure of the oxide layer. It can also be used as an indicator for identifying the onset of the fatigue failure. © 2013 American Institute of Physics. [<http://dx.doi.org/10.1063/1.4793488>]

I. INTRODUCTION

Nickel-titanium shape memory alloys (NiTi SMAs) are well known for their unique functional properties, the one-way effect and pseudoelasticity.¹ With regard to biomaterials, NiTi-based alloys are used as stents, orthodontic arch wires, and filters, etc. For these applications, good mechanical properties (such as fatigue resistance, large reversible strain, and high tensile strength) and biocompatibility (i.e., non-toxicity and corrosion resistance in a body environment) are required.

When a stent is implanted into the human body, it is subjected to static and cyclic mechanical loading. Hence, an understanding of the structural fatigue behavior becomes a necessity. Various methods, like uniaxial (pull-pull) fatigue testing, rotating cantilever bending testing, and bending rotation fatigue testing have been used to assess the fatigue behavior of NiTi.² Miyazaki *et al.*³ introduced bending rotation fatigue (BRF) as a powerful for fatigue life assessment of NiTi SMA wires. Tobushi *et al.*⁴ examined the low-cycle fatigue behavior of NiTi wires under BRF conditions in different environments at different test temperatures. Duerig *et al.*¹ emphasized the importance of studying fatigue loading on NiTi components used in medical applications. Eggeler *et al.*² described the structural and functional fatigue of NiTi shape memory alloys and highlighted the need for further system-

atic studies to understand various parameters that govern the fatigue life. The structural fatigue of pseudoelastic NiTi shape memory wires was examined by Wagner *et al.*⁵ They investigated the influence of wire diameter and rotational speed on the fatigue behavior in various media. It was shown that the fatigue life is independent of the wire diameter and rotational speed, when BRF experiments were conducted at a constant temperature, i.e., in oil instead of air. A systematic study on BRF was performed for NiTiCr alloys, which are normally used in medicine as retriever devices, dental- and guide wires.⁶ The publications cited above are not only scientifically interesting, but they also show the need for a proper understanding of all aspects of NiTi fatigue, which is related to the structural integrity of life saving implants.

Apart from the mechanical and functional properties, the corrosion resistance and biocompatibility of NiTi alloys are also important.⁷ Corrosion of NiTi has been studied extensively.^{8,9} The influence of mechanical loading on the corrosion properties has also been considered.¹⁰ NiTi wires loaded up to 4% tensile strain showed no changes in localized corrosion behavior.¹⁰ The effect of various degrees of deformation (compression) on the corrosion resistance of NiTi was investigated by Montero-Ocampo *et al.*¹¹ The compressive deformation improved the corrosion properties of the material. Huang *et al.*¹² investigated the effects of pH-values and tensile stress on the corrosion resistance of as-received NiTi wires in artificial saliva. Shabalovskaya⁷ pointed out that the electrochemical behavior of the wires subjected to

^{a)} Author to whom correspondence should be addressed. Electronic mail: nlakshman@iitm.ac.in.

bending may differ from that subjected to a tensile load. It has to be mentioned that, even though the mechanical (uniaxial) and electrochemical behavior have been addressed independently, there are only very few *in situ* studies bridging the gap between these two fields.^{13,14} This brief review characterizes electrochemical behavior under the simple loading conditions. Being well aware that the design of such equipment to study simultaneously the mechanical and electrochemical behavior would be challenging, here we address the interplay of fatigue and electrochemical properties of NiTi wire. Fatigue¹⁵ and corrosion¹⁶ are both surface dependent processes and, therefore, it is important to study these combined effects on material integrity. Leinenbach *et al.*¹⁷ suggested that the surface damage due to fatigue can be monitored by following the corrosion potential (E_{corr}) and the corrosion current (I_{corr}) (steady-state conditions) in an integrated electrochemical cell. However, so far, the influence of fatigue on the electrochemical behavior and corrosion parameters, such as break down potential etc., was not yet properly characterized.

The electrochemical behavior under simple bending conditions and under a superimposed cyclic loading (fatigue) can be easily followed. Here, we report on the design and fabrication of an *in situ* BRF test rig with an integrated electrochemical cell. The design of this novel test rig and preliminary results are presented.

II. FABRICATION OF AN *IN SITU* BENDING ROTATING FATIGUE RIG

A. Instrument details

1. Concept and design of the bending rotation fatigue (BRF) test rig

In a BRF experiment, a wire of certain diameter (d) is bent into a semi-circular shape (radius of curvature: R) and forced to rotate by a motor attached to one end.¹⁸ In a simplified mechanical model, the strain in the cross section of the wire is a linear function of the distance from the neutral axis ($y = 0$). The relation between the strain amplitude and the two geometrical parameters d and R is given in Eq. (1).

$$\varepsilon_a = \frac{d}{2R}. \quad (1)$$

Details of the stress and strain distribution across the wire and the influence of experimental parameters on the strain amplitude, are described in Ref. 18.

In the present study a BRF test rig was designed as described previously. However, an electrochemical cell was integrated into the BRF rig, as illustrated in Figure 1. The BRF test rig consists of a height-adjustable vertical base plate (1), to which other components are attached. Arrow 2 points to the bent NiTi wire. The rotating wire was connected to the working electrode (WE) of the potentiostat using a plate contact normally used for relay switches, arrow 3. This contact method worked well for our rotating wire specimens. An inductive proximity sensor (arrow 4) counts the number of cycles and allows to measure the rotational speed. The cycle number is displayed on a small screen highlighted by arrow 5. The rotating wire is attached to a flexible motor shaft, which

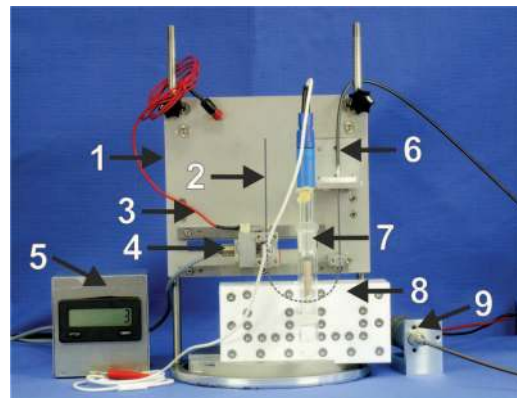


FIG. 1. Photograph showing the complete setup of the *in situ* bending rotation fatigue test rig. (1) BRF base plate, (2) wire specimen, (3) working electrode, (4) inductive sensor, (5) tachometer/counter, (6) flexible motor shaft, (7) reference electrode, (8) electrochemical cell, and (9) DC motor.

is connected to a DC motor (Bühler Motor GmbH), arrow 9. The electrical motor is controlled by a DC power supply (Votcraft). The setup shown in Figure 1 minimizes the interference of electromagnetic noise generated by the motor with the electrochemical measurements. It has to be mentioned here that the wire (WE) was electrically isolated from the motor by inserting a polytetrafluoroethylene (PTFE) cap onto the spindle of the motor shaft. The electrochemical cell (arrows 7, 8) is coupled with the BRF rig as shown in Figure 1.

2. Design of the electrochemical cell and electrochemical interfacing

The design of the three-electrode electrochemical cell is complicated by the fact that the specimen is a bent wire and it continuously rotates. In order to successfully interface the electrochemical cell with the rotating wire and to obtain meaningful results the following conditions have to be satisfied:

- (1) The electrolyte has to be confined to a volume, which allows performing local electrochemical measurements at the point of maximum mechanical load.
- (2) The electrochemical cell has to allow good access for electrochemical measurements, it must be leak-free and it should not interfere with the free rotation of the wire. The cell design must allow studying wire with different bending radii and wire diameters.
- (3) The cell must allow integrating a three-electrode system (reference-, counter-, and working electrode) with proper positioning of all electrodes. The setup must also ensure that the electrodes do not suffer mechanical damage during BRF testing.
- (4) The electrochemical/mechanical test rig must be isolated from external electromagnetic fields, in order to avoid disturbance of the sensitive electrochemical measurements.

Figure 2 shows the elements of the electrochemical cell. The front plate (arrow 1) and the base plate (arrow 2) are made from inert PTFE. The dimension of the front plate is 150 mm

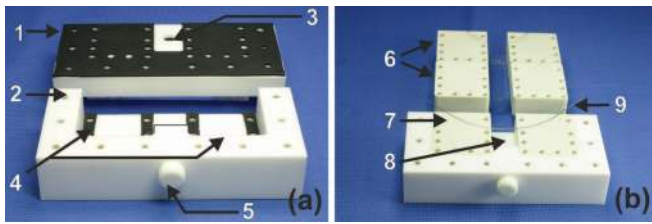


FIG. 2. Details of the electrochemical cell. (a) Front plate with rubber seal (1), cell base plate (2), provision for reference electrode (3), U shaped cavities for inserts (4), electrolyte outlet (5). (b) Cell base plate with inserts (6) for different bending radii, mounted insert ($R = 60$ mm) (7), electrolyte reservoir (8), wire sample (working electrode) (9).

$\times 15$ mm $\times 70$ mm. A circular hole (diameter: ≈ 7 mm, arrow 3) in the front plate allows to position the reference electrode through a luggin capillary. The system was designed to ensure a smooth insertion of the luggin capillary without leakage of the electrolyte. The dimension of the base plate (arrow 2) is 150 mm \times 30 mm \times 70 mm. The base plate actually has a geometry, which was manufactured with a double U-shape (arrow 4). The cavities are separated by a rectangular block with a height of 10 mm and a width of 20 mm. It acts as the base of the reservoir for the electrolyte, when the front plate is attached to the basis. A hole of 6 mm in diameter was made at the bottom of this block, so that samples of the electrolyte can be taken (arrow 5). The rectangular cavities are fitted with exchangeable inserts (arrows 6, 7). Three sets of inserts were fabricated from a glass-fiber reinforced PTFE, as shown in Figure 2(b). The dimensions of the inserts are 45 mm \times 19 mm \times 50 mm. Semi-circular-shaped grooves were machined into the front side of each insert, so that the wires can run at a well-defined bending radius of 30, 45, or 60 mm inside the grooves. The depth of these grooves was slightly greater than the wire diameter (0.8 mm), allowing for the free rotation of the wire. It is worth mentioning that a stagnation of electrolyte might cause a crevice type of corrosion during the electrochemical testing. However, the hydrophobic nature of PTFE and the bend geometry of the groove assure that there is no significant electrolyte stagnation. A chemically inert fluoro rubber (FPM or Viton) material was sandwiched between the base and front plate. This acts as a sealant and prevents the leakage of electrolyte. Chemically inert screws were used in order to assemble the base and front plate together.

III. EXPERIMENTAL EXAMPLES

Commercial binary NiTi (50.7 at. % Ni) SMA wires (Memry GmbH, Weil am Rhein, Germany) with a diameter, $d = 0.8$ mm were used as specimens. The phase transformation temperatures (PTT) of as-received NiTi wires were M_s : -45 °C, M_f : -127 °C, A_s : -15 °C, and A_f : 22 °C. For the experiments presented here, wires were bent into a semi-circular shape with a bending radius $R = 30$ mm, corresponding to an equivalent strain of 1.33% at the point of maximum bending. The test frequency was varied in the range of 0.5–1.25 Hz. The exposed sample area was 0.5 cm². Ag/AgCl (3M KCl) and Au were used as reference and counter electrodes, respectively. All potentials are given with respect to this reference

electrode at room temperature. The test solution, 0.9% NaCl was prepared using analytical-grade NaCl (J. T. Baker) and double-distilled water (J. T. Baker). The electrochemical measurements were performed with an Ivium potentiostat (Ivium Technologies IviumStat XR). In the case of *in situ* open circuit potential (OCP) transient behavior the OCP was measured until failure of the wire. For polarization experiments (*ex situ* and *in situ*), the open circuit potential was measured for 60 min to assure that the system attained a steady state condition. Subsequently, the polarization curves were recorded by gradually increasing the potential, starting from a value of 100 mV below the OCP on the cathodic side to a maximum value of 1 V on the anodic side, at a scan rate of 1 mV s⁻¹.

A. *Ex situ* experiment: Influence of pre-fatigue on the localized corrosion behavior

In the first experimental example, the test rig is being used as an *ex situ* tool to study the influence of fatigue on the corrosion behavior and vice versa. Here, we describe the influence of pre-fatigue on the localized corrosion behavior of pseudoelastic binary NiTi wires.

It is well known that corrosion parameter such as the E_{br} exhibits a wide scatter for NiTi.¹⁹ Therefore, a careful repetition of experiments is required. All of our pre-fatigued wires were subjected to 4000–6000 mechanical cycles in ambient air, using the bending rotation fatigue setup as described above. The polarization behavior shows a significant difference in the break down potential (E_{br}), while the corrosion potential (E_{corr}) and the magnitude of the passive current density (i_p) are quite similar. The average breakdown potential for pre-fatigued wires is 270 mV, which is 40 mV lower than that of a wire in the as-received condition (310 mV). As an example, Figure 3 compares the potentiodynamic behavior of a NiTi wire in the as-received and in a pre-fatigued (5120 mechanical loading cycles) condition. The difference between the two conditions suggests a certain influence of the fatigue loading on the breakdown potential. A possible explanation could be that the stability of the oxide layer on the surface is influenced by cyclic mechanical loading. Further cyclic polarization experiments are required to substantiate

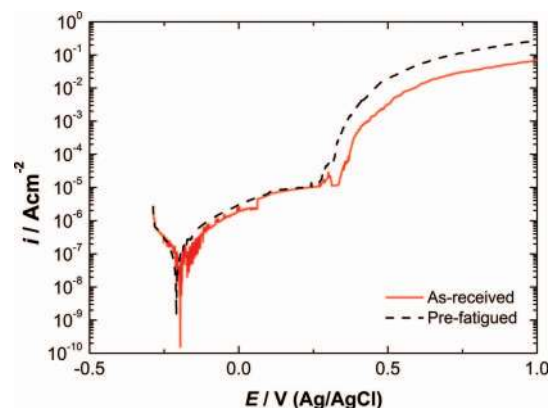


FIG. 3. Comparison of the linear polarization behavior of an as-received and a pre-fatigued NiTi wire. The pre-fatigued wire was subjected to 5120 BRF cycles.

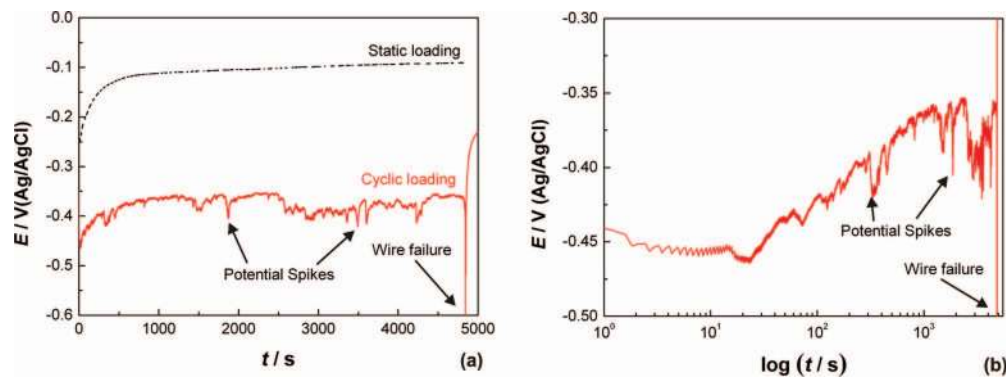


FIG. 4. (a) Comparison of the *in situ* open circuit potential transient behavior for NiTi wires under static bending conditions and subjected to cyclic rotational loading. (b) OCP as a function of $\log(t)$ for a wire under BRF loading.

this observation. However, it has to be mentioned here, that the proposed setup allows performing such studies quite easily, which would be impossible otherwise without removal of the specimen. The surface modification in terms of roughness changes occurring due to fatigue loading could also influence the corrosion behavior, however this is not the focus of the current study.

B. *In situ* open circuit potential transient studies

For the second experimental example, *in situ* testing was performed. The bent wire was subjected to a cyclic rotational loading with a frequency of 1.25 Hz (75 rpm). The selected rotational speed corresponds to that of a typical cyclic loading of a stent in the human body ($f = 1$ Hz).¹

Figure 4(a) compares the variation of OCP transients for the wires exposed to static (bending) and cyclic loading conditions (bending rotation until failure). In terms of the OCP values, the wires subjected to pure static bending appear to be comparatively nobler than the wires subjected to cyclic loading. In all of our experiments, a downward shift of the OCP was observed, when the rotation of the wire was switched on. A possible reason for this rapid shift in OCP could be external disturbances caused by the activation of the DC power supply and/or disturbances (current leakage/electromagnetic noise) caused by the electric motor. However, interferences, if any, were avoided by electrically insulating the wire (working electrode) from the motor spindle (PTFE cap) and by separating the motor from the electrochemical cell (flexible shaft) and cannot contribute to this downward shift. Another possible explanation could be the influence of the rotating wire, which might introduce hydrodynamic conditions during the electrochemical measurements. However, the rather low rotational speed should not significantly lower the OCP. Therefore, this difference in OCP is due to multiple failures of the oxide layer during rotation. It should be mentioned here, that we do not discuss the changes in OCP magnitude, but rather concentrate on the transient features. In both cases the potential moves upwards, which indicates the formation of a stable surface oxide layer. A closer look at the curves in Figure 4(a) reveals that, under static conditions, the potential shift is quiet smooth and shows no potential spikes (potential change). On the contrary, multiple, distinct potential spikes can be observed at random intervals for cyclic loaded

wires. The magnitude of the potential spikes is in the order of 40–60 mV. This could be associated with the failure and repassivation of the oxide layer. Finally, it can be observed in Figure 4(a) that after approximately 4800 s (which corresponds to roughly 6000 mechanical cycles) the potential drastically decreases with subsequent structural failure of the wire. The potential drop is most likely associated with the failure of the oxide layer prior to fatigue failure, because the wire failed exactly when the potential was at the minimum value. Once the wire fails, the potential shifts upwards, indicating the repassivation of the wire. The spikes in the potential curve become clearer and more distinct, when plotted as a logarithmic function of time ($\log t$), as shown in Figure 4(b). An in-depth analysis of the microstructural changes associated with the variation of the OCP will be the scope of future work.

It can be seen that the test rig is designed such that it allows observing the variation of OCP during cyclic loading and predicting the instance of fatigue failure. The average number of cycles for structural failure under these conditions was approximately 5600 cycles.

C. *In situ* potentiodynamic polarization studies

For *in situ* polarization studies, the bent wires were superimposed by a cyclic rotational load at a frequency of 0.5 Hz (30 rpm). Figure 5 shows that the polarization curve exhibits a very low passive current density in the order of a

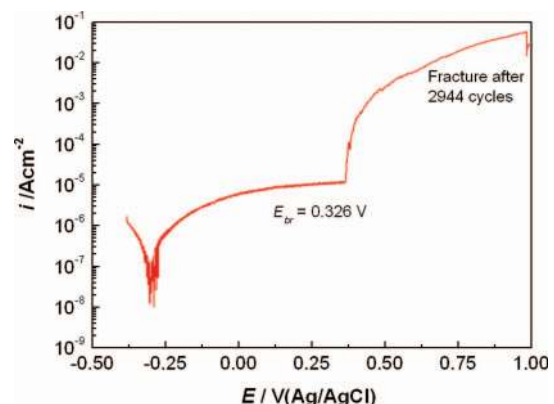


FIG. 5. *In situ* polarization behavior of a NiTi wire subjected to bending rotation fatigue. Structural failure occurred after 2944 cycles.

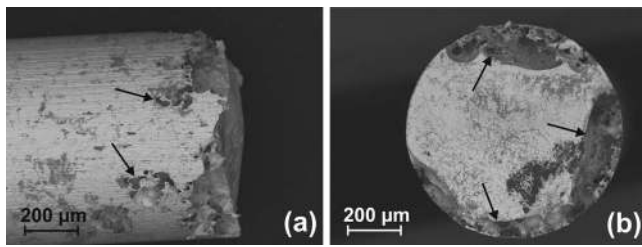


FIG. 6. SEM micrographs of a NiTi wire after *in situ* linear polarization experiments showing damage due to localized corrosion. (a) Wire surface showing pits indicated by arrows. (b) Fracture surface featuring large pits on the outer edges leading to corrosion assisted fatigue failure.

few microamperes and a distinct breakdown potential (E_{br}) of 330 mV.

It is known from previous experiments (results not shown here) that in the absence of corrosive conditions (medium, potential) the wires reach a fatigue life beyond 6000 mechanical cycles. However, when the wires are subjected to conditions which combine corrosion and fatigue, the average structural failure occurs much earlier (2944 cycles). The resulting surface morphology and the fracture surface of such a wire are shown in Figure 6. Pits formed on the surface of the wire due to localized corrosion are indicated by arrows, as presented in Figure 6(a). The influence of corrosion on the fatigue failure can also be observed on the fracture surface in Figure 6(b). It seems that the circumferential area is prone to severe pitting. As a result of localized pitting, in combination with the cyclic mechanical loading, the fatigue life of the wires decreases by more than 50%. The scanning electron microscopy (SEM) observations indicate that pits, which originate on the surface, tend to grow inwards resulting in the reduction of the effective load bearing area. The pits might act as crack initiation sites for early fatigue failure.

IV. CONCLUSIONS

An *in situ* bending rotation fatigue test rig, integrating an electrochemical cell was designed and fabricated. It features a three-electrode setup and various bending radii, and wire diameters can be tested under different sets of parameters. The versatility and the capability of the novel rig were demonstrated by performing *ex situ* and *in situ* experiments. *Ex situ* experiments showed that the pre-fatigue of NiTi wires reduces the breakdown potential (E_{br}). *In situ* experiments allow observing oxide layer damage and repassivation, which occur during cyclic mechanical deformation. The OCP transient can be studied and it becomes possible to predict the exact time/cycle of structural fatigue failure (even before sam-

ple breakage). The test rig can be used to examine the corrosion behavior (E_{corr} and I_{corr}) under steady-state conditions. In addition, it is possible to perform other electrochemical experiments (i.e., polarization studies), while the material is subjected to cyclic mechanical loading. The number of cycles until structural failure is being drastically reduced, when corrosion and fatigue are combined due to the formation of pits acting as crack initiation sites.

Future improvements of our *in situ* test rig will incorporate temperature control to the electrochemical cell, i.e., for running experiments at physiological conditions (37 °C). In addition, a LabVIEW software-based interface between the test rig and the potentiostat will allow for automation of the setup.

ACKNOWLEDGMENTS

The authors acknowledge funding by the German Research Foundation (Deutsche Forschungsgemeinschaft, DFG) and the State of North Rhein-Westphalia through projects T3 and Z of the Collaborative Research Center SFB 459 (Shape Memory Technology). We thank C. Gramann and J. Hartung from the faculty workshop of the Ruhr-Universität Bochum for his work, discussion, and inputs and M. Bienek for his help with the electrical setup.

- ¹T. Duerig, A. Pelton, and D. Stoeckel, *Mater. Sci. Eng. A* **273–275**, 149 (1999).
- ²G. Eggeler, E. Hornbogen, A. Yawny, A. Heckmann, and M. Wagner, *Mater. Sci. Eng. A* **378**, 24 (2004).
- ³S. Miyazaki, K. Mizukoshi, T. Ueki, T. Sakuma, and Y. Liu, *Mater. Sci. Eng. A* **273–275**, 658 (1999).
- ⁴H. Tobushi, T. Nakahara, Y. Shimeno, and T. Hashimoto, *Trans. ASME* **122**, 186 (2000).
- ⁵M. Wagner, T. S. Sawaguchi, G. Kaustraeter, D. Hoeffken, and G. Eggeler, *Mater. Sci. Eng. A* **378**, 105 (2004).
- ⁶M. Frotscher, J. Burow, P. Schön, K. Neuking, R. Böckmann, and G. Eggeler, *Materialwiss. Werkstofftech.* **40**, 17 (2009).
- ⁷S. A. Shabalovskaya, *Biomed. Mater. Eng.* **12**, 69 (2002).
- ⁸G. Rondelli, B. Vicentini, and A. Cigada, *Corros. Sci.* **30**, 805 (1990).
- ⁹N. Figueira, T. M. Silva, M. J. Carmezim, and J. C. S. Fernandes, *Electrochim. Acta* **54**, 921 (2009).
- ¹⁰G. Rondelli and B. Vicentini, *J. Biomed. Mater. Res.* **51**, 47 (2000).
- ¹¹C. Montero-Ocampo, H. Lopez, and A. Salinas Rodriguez, *J. Biomed. Mater. Res.* **32**, 583 (1996).
- ¹²H. H. Huang, *J. Biomed. Mater. Res. A* **66**, 829 (2003).
- ¹³C. Hessel, J. Frenzel, M. Pohl, and S. Shabalovskaya, *Mater. Sci. Eng., A* **486**, 461 (2008).
- ¹⁴L. Neelakantan, B. Schoenberger, G. Eggeler, and A. W. Hassel, *Rev. Sci. Instrum.* **81**, 033902 (2010).
- ¹⁵E. Hornbogen and G. Eggeler, *Materialwiss. Werkstofftech.* **35**, 255 (2004).
- ¹⁶A. W. Hassel, *Minimally Invasive Ther. Allied Technol.* **13**, 240 (2004).
- ¹⁷C. Leinenbach, C. Fleck, and D. Eifler, *Int. J. Fatigue* **26**, 857 (2004).
- ¹⁸T. Sawaguchi, G. Kaustraeter, A. Yawny, M. Wagner, and G. Eggeler, *Metall. Mater. Trans. A* **34**, 2847 (2003).
- ¹⁹R. A. Corbett, in *Medical Device Materials: Proceedings of the Materials and Processes for Medical Devices Conference 2003, Anaheim, California*, edited by S. Shrivastava (ASM International, 2004), Vol. 166.